Int. J. Heat Mass Transfer. Vol. 27, No. 9, pp. 1595–1611, 1984.
Printed in Great Britain

0017 9310/84 $3.00 + 0.00

Structure of thermogravitational convection in flat variously oriented layers of liquid and on a vertical wall

S. S. KUTATELADZE and V. S. BERDNIKOV
Thermal Physics Institute, Siberian Branch of the U.S.S.R. Academy of Sciences, Novosibirsk 90, U.S.S.R.

(*Received* 23 *January* 1984)

FOR AN article in the collection dedicated to the Anniversary of Professor O. Saunders, Royal Society Member, it would be natural to choose a theme close to one of his investigations. In the 1930s he conducted a number of pioneer researches on free thermogravitational convection [1, 2]. During those years one of the present authors was also concerned with the same problem [3]. This problem was returned to in many years, at the Institute of Thermophysics of the Siberian Branch of the USSR Academy of Sciences, owing to the researches of the present authors with A. G. Kirdyashkin and others. Some results of those investigations are presented below.

While studying thermogravitational free convective flows, as with forced flows, there arise a number of fundamental problems [4–6], i.e. the problem concerning the stability of laminar flows and mechanisms of their transition into the turbulent flow; the ambiguity of determining physical parameters being a part of the basic similarity numbers which characterize the problems under consideration for systems with variable physical properties; the unclosedness of the Reynolds system of equations due to appearance of tensor constituents of seeming turbulent tensions, and many others. It is evident that in comparison with the extensive experimental investigations concerning the development of turbulence in forced flows, turbulence in free convective flows has not been sufficiently studied.

The objective reason for it seems to be the fact that the theory of hydrodynamical stability and turbulence has been developed under the influence of the needs of technical hydroaeromechanics, where free convection has been usually considered as a small and unimportant addition. Besides, in the sense of stability, free convective flows are more complicated than the isothermic forced ones, as they may be characterized by a wider spectrum of perturbations. This spectrum includes strongly interacting hydrodynamic and thermal perturbations (the question is thoroughly discussed in refs. [7, 8]).

The velocity field in free convective flows is inseparably linked with the temperature field and must necessarily be measured and analysed simultaneously. It considerably complicates experimental investigations of free convective flows, additionally characterized by small velocities and low frequencies, which makes measurement methods, developed in the studies of forced flows, either unsuitable or in need of considerable additional effort.

In analysing the regularities concerning the near-wall turbulence in forced flows, the canonical object is considered to be a streamlined flat wall. By way of example of a flat isothermic wall (set in parallel with the gravity acceleration vector **g**), overheated with respect to the surrounding medium, one may consider differences and certain analogies regarding the structure (which will be understood as the velocity and temperature fields) of the forced and free convective near-wall flows.

The experimental investigations [9, 10], being among the first of those, where the structure of the thermogravitational flow had been studied, showed that the boundary-layer notion which had been introduced by Prandtl is applicable under conditions of natural convection as well. The main difference occurs with forced convection, the velocity outside the boundary layer approaches the velocity of a travelling flow caused by an external force. Under the conditions of thermogravitational convection, while moving from the plate, the velocity grows and reaches a maximum and then, under the influence of viscosity, drops to zero. In this case, the pressure outside the boundary layer is considered to be hydrostatical and is not specified by the conditions of the external flow. The temperature fields with free and forced convection are similar in form.

Using the existing analogies and general considerations, having been developed by that time and resting upon the boundary-layer concept, Polhausen succeeded in simplifying the system of the basic equations and found the well-known solution for laminar air convection [4, 7, 9]. He used the results of ref. [10]. Then the solutions for media characterized by a wide range of Prandtl numbers, $Pr = \nu/a$, were obtained [4, 11]. Polhausen's solution was widely used in studying the stability of the free convective boundary layer. An extensive reference list concerning this problem and a comprehensive consideration of the investigated results can be found in refs. [7, 8] and in Gebhart's reviews [12, 13]. Some results concerning this problem, obtained at the Institute of Thermophysics of the

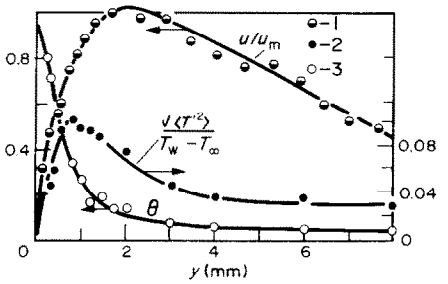

FIG. 1. Mean velocity, temperature and temperature fluctuations intensity profiles, $Pr = 14.5$, $H = 450$ mm, $\Delta T = 11.6°C$, $D = 80$ mm: 1, $Ra = 5 \times 10^{10}$, $x = 363$ mm, $U_m = 34$ mm s^{-1}; 2, 3, $Ra = 5.76 \times 10^{10}$, $x = 381$ mm (according to ref. [21]).

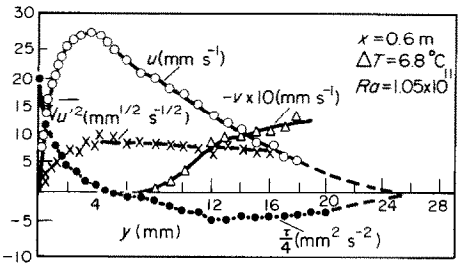

FIG. 2. Distribution of boundary-layer parameters with thermogravitational convection near vertical plate, $Ra = 1.05 \times 10^{11}$, $x = 600$ mm, $\Delta T = 6.8°C$, $H = 700$ mm, $D = 80$ mm, $Pr = 14$–17 (according to ref. [20]).

Siberian Branch of the USSR Academy of Sciences, are contained in ref. [14].

Observations and photographs of liquid, moving near a heated plate, show that a thickening laminar boundary layer develops on its lower part. At a certain distance from the front edge of the plate, the laminar flow is disturbed and a specific thermal turbulence develops. Results of the so far available investigations do not obviously let us trace the genetic relationship between the laminar boundary layer, which has lost its stability, and the developed turbulent one. Therefore, investigations concerning turbulent flow are being carried out largely autonomously.

In earlier [15] and more up-to-date [16] theoretical researches, experimentally obtained regularities of turbulent forced flows are used. In ref. [15], as well as in a number of subsequent researches, the same laws concerning friction and heat transfer, as with forced flows, were assumed to be fulfilled. Experimental research [17–21] does not corroborate it.

As early as 1935, a hypothesis concerning the existence of a viscous sublayer with a constant value of a Reynolds proper number in a turbulent boundary layer on vertical heat transfer surfaces, was put forward [3]. That is to say, a two-layer model of the turbulent free convective boundary layer in the form of a near-wall quasilaminar flow and external jet turbulent movement was suggested. This model was not verified prior to conducting a series of experimental investigations [17–21].

Experimental investigations [17–21] were carried out on two installations, similar in construction and differing only in size. In the first installation, the model of a heated vertical wall, made of a copper plate 450 × 80 × 20 mm, was installed in a container of size 900 × 140 × 110 mm. In the second installation, the dimensions of the plate were 700 × 80 × 30 mm and those of the container 1500 × 500 × 200 mm. Temperature was measured by means of thermocouple probes. Velocity measurements were taken using the stroboscopic visualization technique. The first installation was used in studying the laminar and transition regimes of the flow and taking measurements of statistical characteristics.

With three temperature drops between the isothermic wall and the surroundings ($\Delta T = T_w - T_\infty \approx 7$, 12, and 19°C) and under other similar conditions in the turbulent regime, the velocity (at distances $x = 275$, 400, 500 and 600 mm from the front edge of the plate) and temperature ($x = 263$, 387, 487, and 587 mm) profiles were measured. Some results of these measurements are shown in Figs. 1–3. In Figs. 1

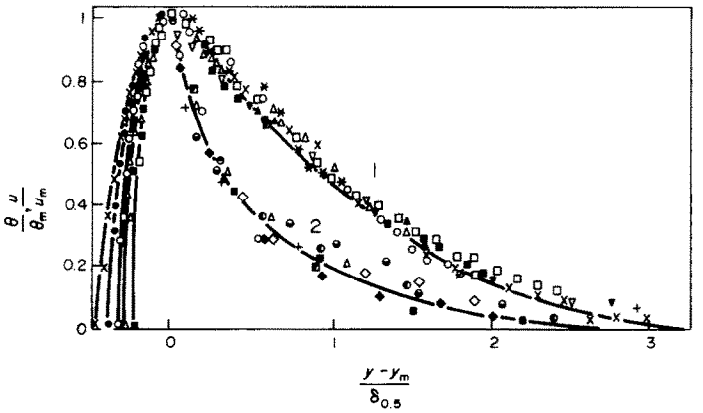

FIG. 3. Profiles of flow averaged velocity longitudinal component and those of mean temperature (2) in turbulent boundary layer with thermogravitational convection near vertical plate, $2 \times 10^{10} < Ra < 4 \times 10^{10}$ (according to refs. [20, 22]).

Table 1

	x (mm)									
	262	387	487	587	262	487	587	387	487	587
ΔT(°C)	12.48	12.41	11.6	11.7	19.78	19.22	19.22	6.96	6.78	6.96
δ_1 (mm)	0.63	0.63	0.65	0.65	0.5	0.51	0.52	0.8	0.82	0.8
G_1	14.4	14.3	15.2	14.8	14.6	15.0	15.9	14.5	15.2	14.5
Re_1	12.6	14.13	13.87	13.63	—	—	—	12.45	13.17	13.45
G_1/Re_1	1.14	1.01	1.1	1.08	—	—	—	1.16	1.15	1.08

and 2, the profiles of the temperature fluctuation intensity and the longitudinal velocity constituent, respectively, are also given. All the results have been obtained with ethanol as a working medium. The obtained results [17–21] enable us to single out three typical domains of the turbulent free convective boundary layer, i.e. the near-wall quasilaminar layer ($y < \delta_1$), the intermediate domain ($\delta_1 < y < y_m$) and the external part of the boundary layer ($y > y_m$). Here m is an index of the parameters for the maximum velocity. The following peculiarities in the near-wall domain have been discovered, i.e.

(1) the averaged flow may be considered as a flat parallel one, as velocity distributions do not depend on the longitudinal coordinate;

(2) the average temperature linearly depends on the coordinate, normal relative to the wall; the boundary of the viscous sublayer can be determined (for $Pr \geqslant 1$) based upon the temperature distribution deviation from this linear dependence;

(3) within the framework of the experimental accuracy, the thickness of the viscous sublayer does not depend upon the longitudinal coordinate x. By using these peculiarities and ignoring the value $\rho u'v'$, the velocity and temperature fields in the near-wall domain can be described by the system of equations [3, 19, 20]

$$\frac{\partial^2 T}{\partial y^2} = 0; \quad \nu\frac{\partial^2 u}{\partial y^2} = -\beta g(T - T_\infty)$$

$$u(0) = 0; \quad u(\delta_1) = u_1; \quad T(0) = T_w; \quad T(\delta_1) = T_1. \tag{1}$$

Hence, for $y \leqslant \delta_1$

$$\frac{T_w - T}{\Delta T} = \frac{T_w - T_1}{\Delta T}\bar{y}; \quad \bar{u} = \bar{y}\left[1 + \frac{G_1}{Re_1}\left(\frac{1}{2} - \frac{T_w - T_1}{6\Delta T}\right)\right] - \frac{G_1}{Re_1}\left(\frac{\bar{y}^2}{2} - \frac{T_w - T_1}{6\Delta y}\bar{y}^3\right) \tag{2}$$

where

$$\bar{u} = u/u_1; \quad \bar{y} = y/\delta_1; \quad G_1 = \beta g \Delta T \delta_1^3/\nu^2;$$
$$Re_1 = u_1\delta_1/\nu; \quad \Delta T = T_w - T_\infty.$$

A comparison of the data from refs. [17–22] shows, while changing Pr 23-fold, $0.7 \leqslant Pr \leqslant 17$, the value $\frac{1}{2} - (T_w - T_1)/(6\Delta T)$ changes by 5%, and the value $G_1 Re_1 = 1.1$–1.5 and does not depend either on the longitudinal coordinate, or on the temperature drop ΔT (Table 1). Re_1 and G_1 have different values for different liquids, however, their relationship is considered to be practically constant. According to the experimental data [17–22]

$$Re_1 = 55Pr^{-0.5} \quad \text{and} \quad G_1 = 60Pr^{-0.5}. \tag{3}$$

From the solution, equation (2), and the ratios, equation (3), for wall friction, one may write

$$\tau_w/\rho = 5.2\frac{(\beta g \Delta T \nu)^{2/3}}{Pr^{1/6}}. \tag{4}$$

Using the experimental data and the integral momentum relation

$$\frac{\partial}{\partial x}\int_0^\delta u^2\,dy = -\tau_w/\rho + \beta g\int_0^\delta (T - T_\infty)\,dy \tag{5}$$

wall friction (Table 2) and its distribution across the boundary layer (Fig. 2) were estimated [20]. Equation (4) and Table 2 show that the coefficient of friction does not depend on the longitudinal coordinate. The same may be said concerning the heat transfer coefficient. They are respectively equal to

$$\sqrt{(\tau_w/\rho)}\frac{x}{\nu} = 2.27G_x^{1/3}\,Pr^{-1/2} \tag{6}$$

and

$$Nu_x = 1.7G_x^{1/3}\,Pr^{-1/6}. \tag{7}$$

Table 2

	x (mm)						
	262	387	487	587	387	487	587
ΔT(°C)	12.48	12.41	11.6	11.7	6.96	6.78	6.96
τ_w/ρ (mm s^{-2})	107	116	110	107	75	75.5	79
$\frac{\tau_w}{\rho(g\beta\Delta T)^{2/3}}$	3.2	3.45	3.37	3.28	3.12	3.2	3.3

In the external part of the turbulent boundary layer, the following peculiarities inherent in the free turbulent jets were discovered, i.e.

(1) that the thickness of the external part of the boundary layer is a linear function of the longitudinal coordinate;

(2) that the gradient of the average velocity along the cross coordinate is constant in most of the domain;

(3) that the value of the intensity of the fluctuations appears to be constant in most of the domain.

By representing the velocity and the temperature profiles in the external part of the boundary layer by means of the coordinates $u/u_m, (y-y_m)/\delta_{0.5}$ (as accepted while analysing jet flows) and $\theta/\theta_m, (y-y_m)/\delta_{0.5}$, it was found that they may be considered as self-similar [20] (Fig. 3). Here $\delta_{0.5} = y_{0.5} - y_m$, $y_{0.5}$ corresponds to the velocity value $u = 0.5u_m$.

Using the above-mentioned peculiarities and ignoring the friction τ_m/ρ and the members $(\theta v)_m$ and $(uv)_m$, from the integral equations of pulses and energy for the external part of the boundary layer

$$\frac{\partial}{\partial x}\int_{y_m}^{\infty} u^2\,dy - \int_{y_m}^{\infty} \beta g\theta\,dy + \frac{\tau_m}{\rho} - (uv)_m = 0 \quad (8)$$

and

$$\frac{q_m}{\rho C_p} = \frac{\partial}{\partial x}\int_{y_m}^{\infty} u\theta\,dy - (v\theta)_m \quad (9)$$

the ratios u_m and θ_m for the estimate of the maximum velocity, i.e.

$$u_m \Big/ \left(\frac{q_0 \bar{x}\beta g}{\rho C_p}\right)^{1/3} = C_1; \quad \theta_m(\beta g\bar{x})^{1/3} \Big/ \left(\frac{q_0}{\pi C_p}\right)^{2/3} = C_2 \quad (10)$$

were obtained [20].

As obtained from experiments [14–18, 20], $C_1 = 2.1$; $C_2 = 16.4$ for liquids with $Pr = 0.7$–17. Here $\bar{x} = x - x_0$, is the longitudinal coordinate read off not from the edge of the plate, but from the coordinate of the fictitious origin of the turbulent boundary layer $x_0 = x_C(1 - \alpha_l/\alpha_T)$. The true origin of the turbulent boundary layer x_C is found experimentally, based upon the distribution of the heat transfer coefficient α according to the height of the plate, i.e. for $Pr \approx 16$, $Ra_C = \beta g \Delta T x_C^3/av = 1.7 \times 10^{10}$ [20].

Statistical characteristics of the velocity and temperature fields were investigated in refs. [18, 21]. The profiles of the RMS values $\sqrt{\overline{u'^2}}$ and those of the absolute mean values $\overline{|u'|}$ for the fluctuations of the velocity longitudinal constituent are considered to be self-similar in the coordinates $\sqrt{\overline{u'^2}}/u_m$; $(y-y_m)/\delta_{0.5}$ and $\overline{|u'|}/u_m$; $(y-y_m)/\delta_{0.5}$, respectively.

The maximum value $\sqrt{\overline{u'^2}} = 0.3u_m$ (Fig. 2). The average absolute values for the velocity fluctuations in most of the boundary layer ($y > y_m$) slightly depend on y. The profiles of the RMS values for the temperature fluctuations show that the greatest value of $\sqrt{\overline{T'^2}} = 0.07\Delta T$ (Fig. 1) and is moved to the wall relative to the maximum value $(u'^2)^{1/2}$. In the $y < y_m$ domain, the following peculiarities of the one- and two-point moments obtained by means of microthermocouples, one of which had been installed on the boundary of the viscous sublayer [18, 20, 21], were observed. The temperature fluctuations turn out to be rigidly correlated according to the coordinate, normal relative to the wall, i.e. the correlation coefficient varies from 1 to 0.7. At the same time, the variance of the temperature fluctuations within the range 0.12 mm $\leqslant y \leqslant$ 0.52 mm changes 30-fold. Time integrals and microscales determined according to the autocorrelation functions are practically equal. The integral L_u and the microscale L_ε, determined on the basis of the spatial correlation function, are also equal and commensurable with the above determined $\delta_{0.5}$ ($L_u = 5.3$ mm and $L_\varepsilon = 5.5$ mm for $\Delta T = 11.3°C$, $x_0 = 365$ mm, and $y_0 = 0.64$ mm). Estimates for the spectral density of the temperature fluctuations (Fig. 4) show that with the temperature drop $\Delta T = 15.5°C$, considered to be a maximum in this series of experiments, the maximum frequency does not exceed 8 Hz. As ΔT grows, the shift of the spectrum into the higher frequencies domain occurs. As fast as one approaches the wall, the spectrum shifts into the lower frequencies domain.

The second actively studied object appears to be the layer of liquid, limited to the height, H, and contained

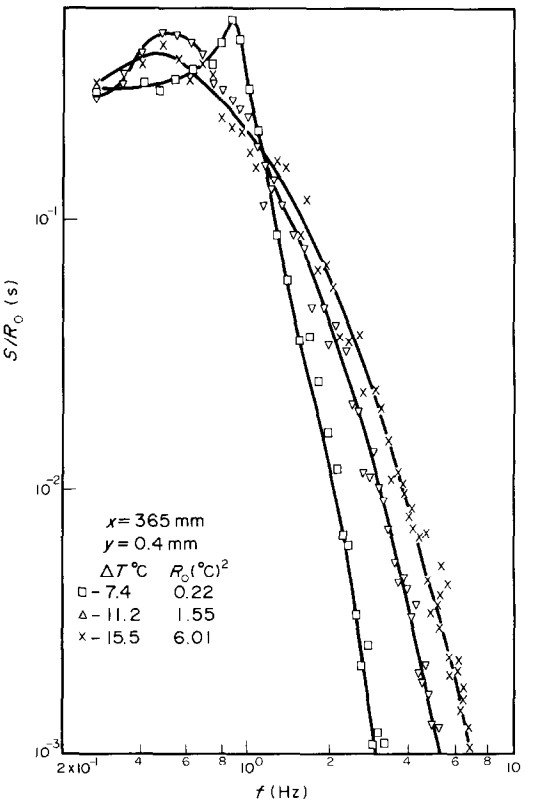

FIG. 4. Dependence of viscous sublayer temperature fluctuations spectral density on temperature drop, H = 450 mm, D = 80 mm (according to ref. [21]).

between two parallel plates, heated up to various temperatures, T_1 and T_2, $T_1 > T_2$, and inclined at a certain angle α to the direction of the force of gravity. Experimental investigations concerning the structure of the main flow in the laminar regime [23–27], theoretical and experimental investigations, concerning the stability of the laminar flow [25, 27–31], as well as experimental investigations, concerning the structure of the flow in the turbulent regime [17, 32–34], were carried out.

To approximately describe the thermogravitational flow, practically realized in the considered system (in the laminar regime), two models were suggested. The well-known system of equations for thermal convection, provided that the dimensionless variables have been introduced, as the Boussinesq approximation, can be written as

$$\frac{\partial \mathbf{V}}{\partial t} + G(\mathbf{V}\cdot\nabla)\mathbf{V} = \nabla P + \nabla^2\mathbf{V} + T\cdot\gamma \tag{11}$$

$$\frac{\partial T}{\partial t} + G(\mathbf{V}\cdot\nabla)T = \frac{1}{Pr}\cdot\nabla^2 T \tag{12}$$

$$\nabla\mathbf{V} = 0. \tag{13}$$

Here $G = \beta g \Delta T L^3/\nu^2$, and L (the distance between the plates), L^2/ν, ΔT, $\beta g \Delta T L^2/\nu$, and $\rho_0 \beta g \Delta T \cdot L$ have been chosen as distance, time, temperature, velocity, and pressure units, respectively. In a cavity of dimensions $L \times D \times H$, the condition $D/L \gg 1$ is sufficient for one to consider the problem as being flat (in the x, y coordinates). The flow will be flatly parallel for $h = H/L \to \infty$ only (infinitely long layer). Taking into account simplifications and the boundary condition

$$\mathbf{V} = 0 \text{ for } y = \pm 1/2;\ T = \pm 1/2 \text{ for } y = \pm 1/2 \tag{14}$$

the system, equations (11)–(13), has the well-known solution [4]

$$u_0 = -(y - 4y^3)/24 \tag{15}$$

$$T = -y. \tag{16}$$

Equations (15) and (16) describe properly the flow with Rayleigh numbers $Ra = G\,Pr \lesssim 10^4$ for $h < \infty$. Such a flow regime with a linear temperature profile was referred to as the conduction regime [16].

As shown in refs. [24–26, 35–39], for $Ra \gtrsim 2 \times 10^4$, with such dimensions of layers that are typically realized in experimental investigations, the laminar conduction regime changes to the other laminar regime, i.e. the boundary-layer regime. This regime may be characterized by a low mobile core in the center of the cavity and development of dynamical and thermal boundary layers near the walls. It has been experimentally shown that the characteristic feature of this regime turns out to be the existence of a constant temperature gradient A in the core [24–26, 35–39]. Having been measured in units of $\Delta T/L$, this gradient satisfies the simple ratio

$$A = (0.5\text{–}0.6)h \tag{17}$$

which does not practically depend on the values of Pr, Ra and the angle of inclination, α (Fig. 5).

In ref. [35], it was shown for the first time that this regime could be properly described by the solutions of the problem, concerning free convection in an infinite slot with a constant longitudinal temperature gradient on the walls (complementary to the cross temperature difference) [39], i.e.

$$T = \pm\tfrac{1}{2} + Ax \quad \text{for} \quad y = \pm\tfrac{1}{2}. \tag{18}$$

The solutions obtained in ref. [39] (for $\alpha = 0$) have been generalized for the case of inclined layers and checked experimentally in refs. [26, 37]. The solutions, obtained in refs. [26, 37], have been refined in ref. [27], taking into account the finiteness of the correction $A \tan\alpha$, and are as follows:

$$\bar{u} = [K_2 \cos(my)\sinh(my) - K_1 \sin(my)\cosh(my)]/2m^2 \tag{19}$$

$$\bar{T} = [K_1 \cos(my)\sinh(my) + K_2 \sin(my)\cosh(my) - Ay\sin\alpha]/\cos\alpha \tag{20}$$

$$K_1 = \frac{1 - A\tan\alpha}{\cos(m) - \cosh(m)} \cos\left(\frac{m}{2}\right)\sinh\left(\frac{m}{2}\right)\cos\alpha \tag{21}$$

$$K_2 = \frac{1 - A\tan\alpha}{\cos(m) - \cosh(m)} \sin\left(\frac{m}{2}\right)\cosh\left(\frac{m}{2}\right)\cos\alpha \tag{22}$$

$$A\,Ra\cos\alpha = 4m^4. \tag{23}$$

In ref. [27], the independent parameter characterizing the main flow, was considered to be the number m, not h, as it had typically been. For $A \to \infty$ ($m \to 0$), equations (19) and (20) change to equations (15) and (16).

The existence of a conduction regime in a vertical air layer was shown in ref. [40] with the help of the interferometric method. During the growth of the temperature drop $\Delta T = T_1 - T_2$, the appearance of the temperature gradient (vertical) was observed. It has

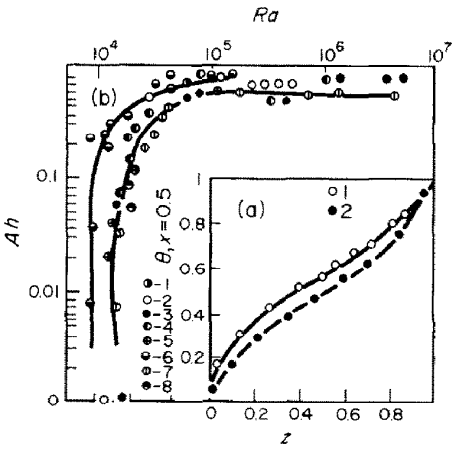

FIG. 5. Dependence of layer longitudinal gradient on Ra (according to refs. [26, 36]).

been shown in ref. [24], by means of experiments with vertical layers of ethanol, that for $Ra < 1.5 \times 10^4$, profiles (15) satisfactorily coincide with the experimental profiles in form and amplitude in the central part of the cavity $0.2 \lesssim X/H \lesssim 0.8$. For $Ra = 2 \times 10^4 - 5 \times 10^5$, the experimental velocity and temperature profiles can be described by equations (19) and (20), respectively, as well as in the domain, considered to be central relative to x, excluding the end-wall parts of the cavity. In ref. [26], in experiments concerning the inclined layers of liquid with stable stratification (we will assume subsequently that $\alpha > 0$), when the temperature of the upper plate T_1 exceeds the temperature of the lower one T_2, the measurements of the velocity and temperature profiles also showed the correctness of equations (19) and (20) in that domain of the parameters Ra, Pr, h, and α, where $A = \text{const.}$ (Fig. 5).

Theoretical investigations of the conditions, concerning the origination and form of secondary flows in layers limited in height, resolve themselves into studying the stability of the profiles, equations (15) and (16) and equations (19) and (20). The results of numerous theoretical investigations concerning the conduction regime, have been systematized in ref. [7].

The flow described by equations (15) and (16), has three types of instability. For all Pr's this flow loses its stability relative to the monotonously growing perturbations of the roll-type, whose axes go along the Z-axis (stationary cross rolls R_1), for which $G_C \approx 8000$, and slightly depends on Pr. For $Pr > 11.4$, there exists an oscillatory branch of instability (travelling waves W), for which, for large Pr's, G_C has the asymptotical dependence $G_C = 8528/\sqrt{Pr}$. For negative inclination

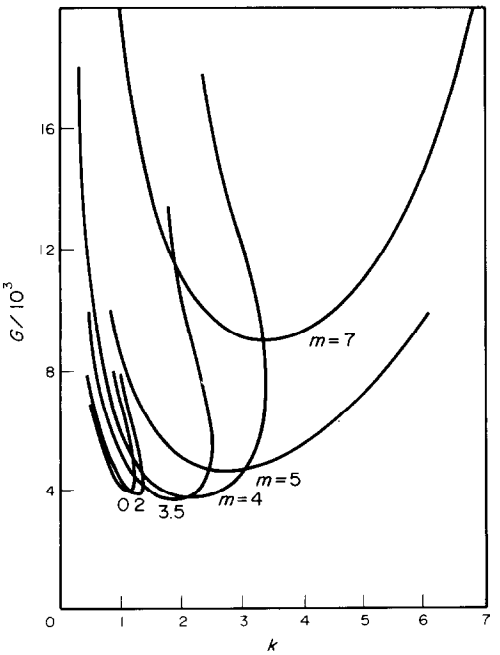

FIG. 6. Family of wave instability (W) neutral curves for $Pr = 15$, $\alpha = 0$ (according to ref. [31]).

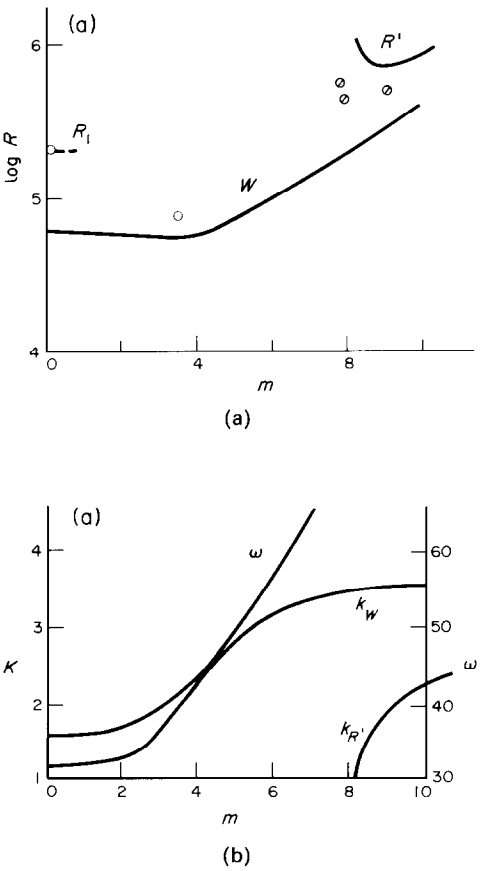

FIG. 7. Dependence of wave instability (W) parameters critical values on m, $\alpha = 0$ (according to ref. [31]).

angles (heating from below) and $Pr > 1$, spatial perturbations, i.e. spiral-type movements, whose axes go in the direction of the main flow (longitudinal rolls R_2), develop earlier than the others. The critical Rayleigh number of these perturbations is associated with the critical number Ra_c of the Bénard problem, i.e.

$$Ra_C = 1708/\sin \alpha.$$

Studying the profiles, equations (19) and (20), with the help of the minor perturbations method allowed us to establish [27, 28, 30, 31], that this flatly parallel model has five types of instability. First of all, there are the three types of instability existing in the conduction regime ($m = 0$), which may be expanded into the $m > 1$ domain, i.e.

(1) the R_1 instability;

(2) the W instability (the non-stationary type instability due to the interaction of thermal and hydrodynamical perturbations, which generates the travelling thermoconvective wave);

(3) the stationary type longitudinal orientation instability (the Bénard type, while heating from below), existing in the $\alpha < 0$ domain.

Secondly, there are the instabilities, whose development is associated with the availability of the temperature longitudinal gradient, i.e.

(1) the stationary type cross orientation instability R', existing for large Pr and $m \gtrsim 7$;

(2) the longitudinal orientation instability R_3, occurring while heating from above ($\alpha > 0$).

The R' instability is due to the lower thermal level [27, 31] (v_0) and differs from R_1 in pattern. The pattern of R_1 is hydrodynamical and this vortex track on the boundary of the meeting flows exists even when temperature perturbations are not available. The R_3 instability differs from the longitudinal rolls type instability R_2 in energy balance, i.e. it exits in a steadily stratified (on average) system.

In Fig. 6, a family of neutral curves of the W instability according to ref. [31] is given, the numbers specifying the value of the parameter m. The curves interpolating the values of Ra_C, the wave numbers and the perturbation frequencies are given in Fig. 7 (according to ref. [31]). The conditions, under which secondary flows of the stationary rolls type and those of the travelling wave type, respectively, have been observed, are indicated with points 1 and 2.

It can be seen therefrom, that, with the growth of G, the wave type instability in the whole domain of the values m occurs earlier.

The critical Rayleigh numbers of the R' instability for $Pr = 100$ are presented in Fig. 8 (according to ref. [31]). The critical Rayleigh numbers observed in ref. [25] for stationary secondary flows in a transformer oil layer are marked with points. The behaviour of the critical wave numbers is also shown.

The positions of the wave and stationary (R') type instability domains for a fixed value of the parameter $m = 8$ within the range of Prandtl numbers $5 < Pr < 1000$ are shown in Fig. 9 (according to ref. [31]).

The data in Figs. 6–9 refer to the case, when $\alpha = 0$. In Fig. 10 (according to ref. [27]), the results of a computation for the profiles, equations (19) and (20), with $m = 10$, which show the influence of the angle of inclination on the R' and R_3 instabilities, are presented. For $\alpha \approx 60°$, these instabilities have approximately similar critical values of Ra_C, therefore,

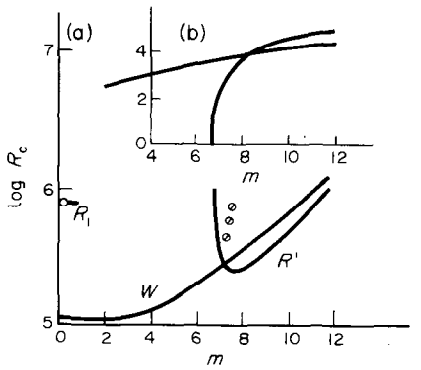

FIG. 8. Dependence of R' instability parameters critical values on m, $\alpha = 0$ (according to ref. [31]).

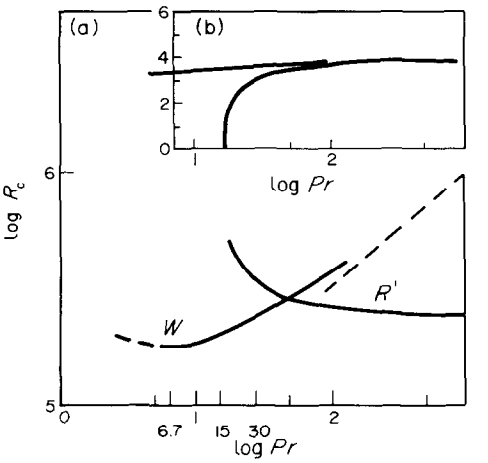

FIG. 9. Dependence of critical Rayleigh numbers and wave numbers of W and R' instabilities on Prandtl number for $m = 8$, $\alpha = 0$ (according to ref. [31]).

the manifestation of both instabilities here appears to be possible.

In Fig. 11 (according to ref. [27]), the experimental and computational results for $\alpha = 70°$ are given. Points 1–5 correspond to the conditions, under which secondary flows of the longitudinal type have been observed, point 6 being the superposition of the cross and longitudinal structures, points 7–9 that of the cross structures. Secondary structures of the longitudinal type can be observed in long layers ($h > 20$), which corresponds to $m < 6.2$. In shorter layers, the cross type structures dominate. Within the given (minor) range of angles of inclination, the influence of the angle of inclination upon the pattern of secondary flows is less pronounced than the influence of the length of the layer.

The development of the above-listed instabilities up to finite amplitude secondary flows and the further development of the flow structure have not been thoroughly investigated. In refs. [17, 32–34], the characteristics of the developed turbulent flow have been investigated for the most part.

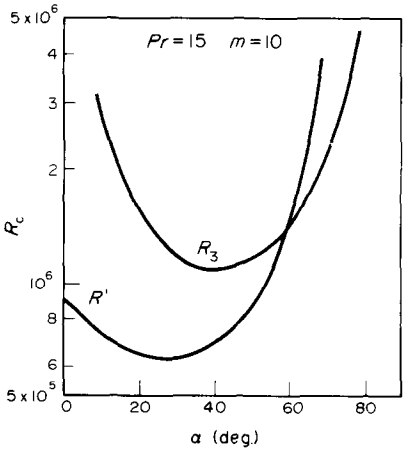

FIG. 10. Longitudinal (R_3) and cross (R') type instability domains in inclined layers, $Pr = 15$, $m = 10$.

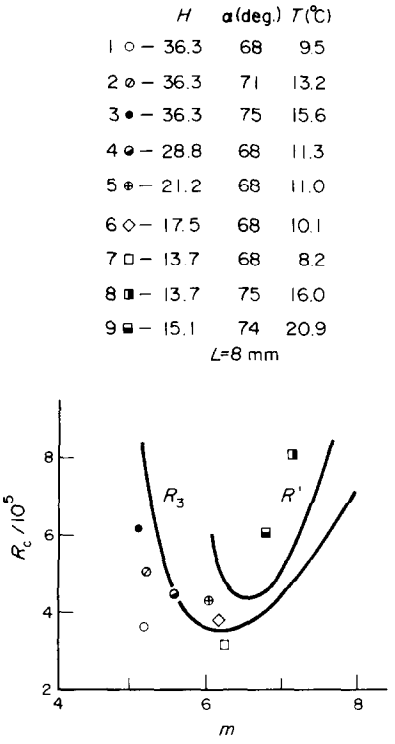

FIG. 11. Longitudinal and cross type instability domains in inclined layer, $\alpha \approx 70°$, $Pr \approx 15$.

Temperature measurements in the middle section of $y = 1/2$ showed that the distribution of the non-dimensional temperature $\theta = (T - T_2)/(T_1 - T_2)$ along the height, for the same ΔT, does not depend on L. For the same L, as the height of the layer and ΔT grow, there appears and develops a zone in the core, where the non-dimensional temperature gradient $(H/\Delta T)(dT_m/dx) \cong 0.36 \pm 0.04$ (Fig. 12). The boundary of the developed turbulent regime of the flow may be determined according to the appearance of the layer of such a zone in the central region. In ref. [32], for $Pr = 16$, $H/L < 26$, this boundary is defined by $Ra_{H,C} = \beta g \Delta T H^3/av \cong 5 \times 10^{10}$. As can be seen from above, the $Ra_L = \beta g \Delta T L^3/av$ criterion is not considered to be determinative in this case [41]. Measurements of the (average) temperature distribution along the y-coordinate, normal relative to the wall, in the constant longitudinal gradient domain showed that the temperature near the wall changes linearly, its value in the core being constant [17, 32]. Processing of these data showed that the dependence of the non-dimensional heat transfer coefficient $Nu_x = \alpha x/\lambda$ on $Ra_x = \beta g \Delta T x^3/av$ turns out to be the same, as with the turbulent thermogravitational convection near the isothermic vertical plate, i.e. $Nu_x = 0.108 Ra_x^{1/3}$ [32]. Estimating the value of the Grashof number for the viscous layer $G_1 = \beta g \Delta T_m \delta_1^3/av$, based upon the thickness of the temperature linear change region and the local temperature drop, showed that it is as important as the turbulent convection of the single plate $G = 15 \pm 5$.

However, stable stratification of liquid outside the boundary layers results in certain differences of the flow pattern in a layer, relative to the flow near the single plate. The intensities of the velocity and temperature fluctuations in the layer are higher than those of the plate. The maximum of the velocity longitudinal constituent is closer to the heat transfer surface, the temperature boundary layer being more drowned in the dynamical one. In ref. [17], the data concerning the behaviour of the profiles of the velocity mean longitudinal constituent on the separate plate, when the temperature drop $\Delta T = T_w - T_\infty = \text{const.}$, and in the vertical layer (Fig. 13), in whose core there exists the longitudinal temperature gradient, were presented. On the basis of these data, $Re_1 = U_m \delta_m/v$ (Fig. 14) were calculated. The values of Re_1 depend on the relative temperature gradient $[d/dx(T/\Delta T)]_y > \delta$ and, at its similar values, are constants which are independent of Ra. It refers to the temperature constant longitudinal gradient domain, within whose range, there exists a quasi-stable, near-wall layer.

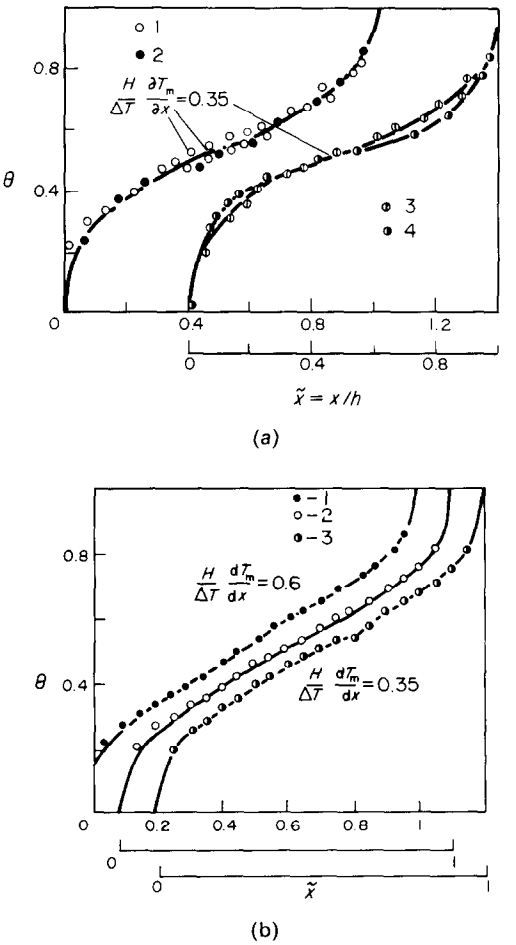

FIG. 12. Non-dimensional temperature profiles in the centre of vertical layer, $y = L/2$, $H = 395$ mm, $L = 45$ mm: 1, $\Delta T = 7.7°C$, $Ra_L = 5.2 \times 10^7$; 2, $\Delta T = 10.2°C$; 3, $\Delta T = 12°C$ (according to ref. [32]).

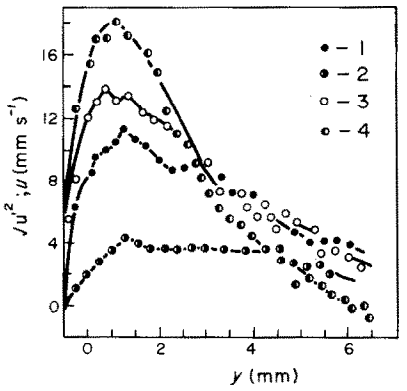

FIG. 13. Profiles of velocity longitudinal component mean (1, 3, 4) and fluctuations RMS values (2) in layer $H = 395$ mm, $L = 49$ mm, $x = 0.5H$. 1, 2, $Ra_L = 10^8$, $\Delta T = 11.3°C$, $T_m = 27°C$; 3, $Ra_L = 1.7 \times 10^8$, $\Delta T = 17.9°C$, $T_m = 31.07°C$; 4, $Ra_L = 3.28 \times 10^8$, $\Delta T = 29.0°C$, $T_m = 39.3°C$ (according to ref. [17]).

In Fig. 13, the profiles of the velocity longitudinal constituent RMS fluctuations are given. Comparison with Fig. 2 shows that the behaviour of the velocity fluctuations in the layer is a repetition of their behaviour on the single plate.

The average velocity profiles for the external part of the boundary layer [in the coordinates u/u_m; $(y-y_m)/\delta_{0.5}$] and the average velocity profiles for the near-wall domain [in the coordinates $(T_1-T)/(T_1-T_m)$; $\bar{y} = G_y^{1/3} Pr^{1/6}$] turn out to be self-similar [32].

Therein the similarity of turbulent flows both in the layer and on the single plate, also manifests itself. Statistical characteristics of the temperature field (one-point moments) in turbulent vertical layers were studied in refs. [33, 34].

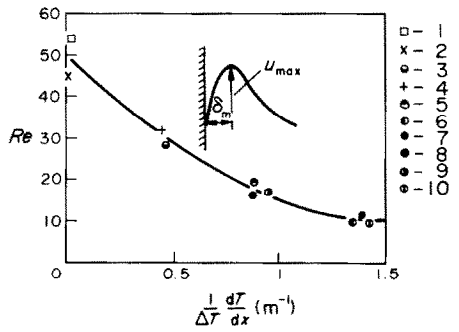

FIG. 14. Dependence of Re_1 on temperature relative to longitudinal gradient $(1/\Delta T)(dT/dx)$. Plate: 1, $Ra_x = 4.83 \times 10^{10}$, $x = 363$ mm, $\Delta T = 11.6°C$, $T_\infty = 29.4°C$; 2, $Ra_x = 2.15 \times 10^{10}$, $x = 275$ mm, $\Delta T = 11.8°C$, $T_\infty = 29.2°C$. Layer: $Ra_L = 8.85 \times 10^8$, $H = 680$ mm, $L = 31$ mm, $\Delta T = 28.8°C$, $T_m = 42.7°C$; 3, $x = 260$ mm; 4, $x = 385$ mm, $H = 395$ mm, $L = 49$ mm, $x = 0.5H$; 5, $Ra_L = 3.28 \times 10^8$, $\Delta T = 29.0°C$, $T_m = 39.3°C$; 6, $Ra_L = 10^8$, $\Delta T = 11.3°C$, $T_m = 27°C$; 7, $Ra_L = 1.7 \times 10^8$, $\Delta T = 14.9°C$, $T_m = 31.07°C$, $H = 395$ mm, $x = 0.5H$; 8, $Ra_L = 1.04 \times 10^7$, $L = 15$ mm, $\Delta T = 31.9°C$, $T_m = 40.8°C$; 9, $Ra_L = 8.45 \times 10^7$, $L = 30$ mm, $\Delta T = 32°C$, $T_m = 40.2°C$; 10, $Ra_L = 4.76 \times 10^6$, $L = 15$ mm, $\Delta T = 16.7°C$, $T_m = 31.8°C$ (according to ref. [17]).

Let the limiting case of the inclined layer, when $\alpha = -90°$, and equations (19) and (20) describe the equilibrium of the horizontal layer, uniformly heated from below, be considered. The critical Grashof numbers G_C considerably depend on Pr. The product $G_C\,Pr$ turns out to be practically constant, being the characteristic feature of the equilibrium thermogravitational stability.

In a horizontal layer of liquid, uniformly heated from below, with the critical value of the temperature gradient, there develops a specific spatial-periodical flow, and so called Bénard cell convection. The spatial form of the developing flow strongly depends upon the conditions on the horizontal boundaries [7]. To date, numerous investigations concerning the boundary of the mechanical equilibrium stability of the below heated layer of liquid under various boundary conditions have been carried out. The problem concerning the mechanisms of selecting the stable forms of the flow and those of further complicating the structure of the flow has been studied to a lesser extent [42–44].

In refs. [45–52], the results concerning mostly the experimental investigations on heat transfer, the structure of laminar cell and turbulent convection, and the evolution of the cell flow spatial form with the growth of Ra, are presented.

The lower boundary of the layer in all the experiments is assumed to be a rigid isothermic copper plate; the ratio of the heat conductivity coefficient of copper to the conductivity coefficient of ethanol, on which the experiments have been conducted, is equal to 2.17×10^3. The upper boundary of the layer in some experiments was rigid and isothermical (copper or mirror glass, the ratio of conductivities being equal to 4.54), in the others it was free. In the latter case, the layer was cooled from above, by means of a transparent heat exchanger, through a gas–air layer. In refs. [51, 52], the horizontal boundaries of the layer were, at the same time, the probes of the heat flow.

For both types of boundary conditions, the characteristic feature of the flow, i.e. as fast as hypercriticality grows, constant qualitative reconstructions and complications of the structural form and the structure of the flow occur, was observed. The process develops in stages, at intervals of Ra or Ra and Ma, within which the flow does not qualitatively change, being clearly observed, i.e. a number of successive perturbations of the stability of the flow, growing more complicated, as fast as Ra grows, can be observed, however, after each successive perturbation of stability, there develops a flow, which preserves the spatial ordering to a great extent, even in the case of its dependence on time.

This peculiarity of the flow was also observed in ref. [53], where, for the most part, the evolution of the spatial form of the thermogravitational flow with the growth of Ra for different Pr's, was studied. It was also the research, where the authors attempted to connect the stages of the development of the flow with the

growth of Ra, with the so-called 'discrete transitions in the heat transfer curves', discovered within a wide range of numbers $Ra \lesssim 2 \times 10^6$ in ref. [54] and pointed out later on in refs. [53, 55–57]. These discrete transitions manifest themselves as a piecewise-linear dependence of the measured heat flow Q on ΔT (in the linear coordinates $Q = f(\Delta T,\ H = \text{const.})$, or in the non-dimensional form $Nu\ Ra = f(Ra)$, whose slope changes at certain Ra_i. Here $Nu = \alpha H/\lambda$ is the non-dimensional heat transfer coefficient (the Nusselt number), α the heat transfer coefficient and λ the thermoconductivity coefficient of the liquid.

The ideological background of refs. [51–57] is considered to be the earlier studies [1, 58], where experimental investigations concerning heat transfer across horizontal layers were begun. Besides, refs. [58] was the first to suggest a determination of the mechanical equilibrium instability boundary with the help of heat measurements. The idea consists in that, during the perturbation of the mechanical equilibrium and the development of the convective flow with $Ra_1 \approx 1700$, for two rigid walls [58], the heat flow constituent convective appears and the above-mentioned dependence of the heat flow on the difference and the temperature undergoes a fracture. In ref. [1], the measurements that had been started in ref. [58], were continued up to $Ra \lesssim 1.5 \times 10^5$, and the second fracture for $Ra \approx 4.7 \times 10^4$, which was interpreted as a transition from the laminar flow to the turbulent one, was discovered. Thereupon in ref. [59], while analysing the experimental results of ref. [60], the alteration of the heat transfer law for $Ra \approx 5 \times 10^5$ was observed and an interpretation of this change as a transition from the turbulence with the laminar boundary layer to the turbulence with the turbulent boundary layer was given.

In ref. [61], where numerical investigations concerning the two-dimensional convection were carried out, this series of transitions was represented as follows:

$Ra_2 = (1\text{–}2) \times 10^4$

(weakly intensive turbulence development);

$Ra_3 = (5\text{–}8) \times 10^4$

(locally high intensity turbulence);

$Ra_4 = (1.6\text{–}2.3) \times 10^5$

(uniformly high intensity turbulence);

$Ra_5 = (4.1\text{–}6.4) \times 10^5$

(beginning of the shear turbulence perceptible influence).

These notions do not conform with the experimental investigations [45–57], whence it follows that turbulence develops much slower, as fast as Ra grows.

The results of refs. [54–57], obtained for large Ra, under various conditions (the measurements were carried out under non-stationary or quasi-stationary conditions, on installations, greatly differing in geometrical form and relative dimensions, i.e. the relationship between the least horizontal size of the layer and its height H) do not yield to generalization and interpretation, by analogy with the results [53].

In refs. [51, 52], the authors attempted to discover the discrete transitions within a wide range of Ra (from the conduction regime to $Ra = 2 \times 10^8$) on an installation with liquid, $Pr \approx 16$ (ethanol), in order to associate these discrete transitions with the evolution of the structure of the flow [45–52], observed as fast as Ra grows. The measurements of the heat flow were carried

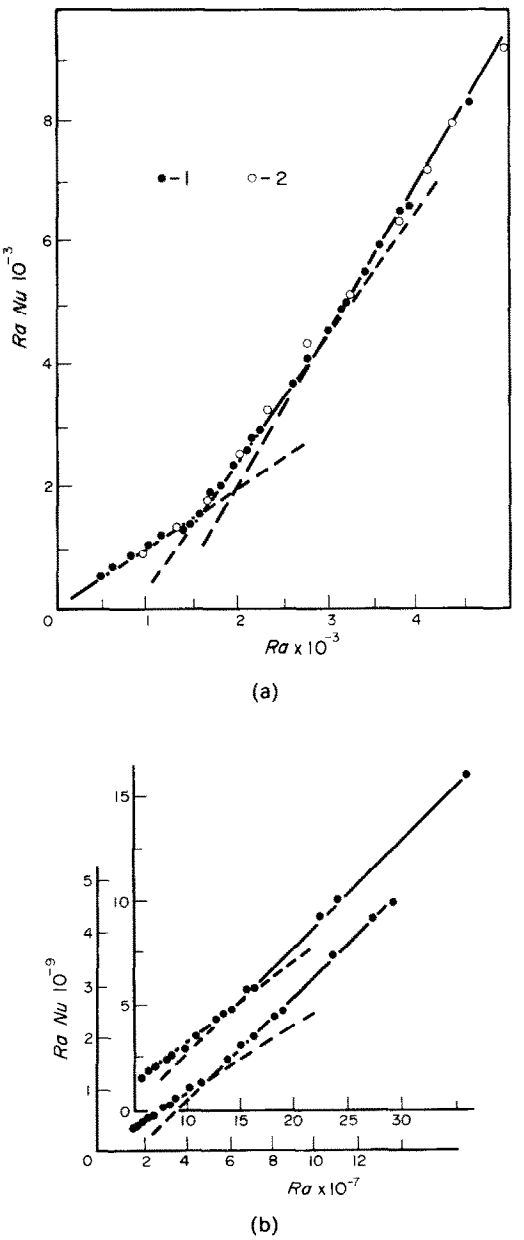

FIG. 15. Dependence of non-dimensional heat flow $Nu\ Ra$ on temperature non-dimensional drop between boundaries of layer Ra.

Table 3

	i						
	1	2	3	4	5	6	7
Ra_i	1.7×10^3	2.65×10^3	6.7×10^3	1.96×10^4	3.9×10^4	6.7×10^4	1.33×10^5
Nu_i	1	1.43	2.1	2.82	3.21	3.85	4.58
$\tan_{i-1,i}$	1	2.21	2.5	3.17	3.61	4.75	5.34

	i						
	8	9	10	11	12	13	14
Ra_i	3.9×10^5	1.0×10^6	3.05×10^6	7.35×10^6	1.39×10^7	5.05×10^7	1.42×10^8
Nu_i	6.15	8	11.5	14.8	17.5	22.4	33.9
$\tan_{i-1,i}$	6.96	9.77	13.1	17.1	20.5	26.9	39.3

out by using upper copper and glass heat exchangers. The horizontal dimensions of the investigated layers were 240×240 mm, $4 \leqslant H/L \leqslant 120$.

In Fig. 15, the dependence of $Nu\ Ra$ on Ra, experimentally obtained in ref. [47], is given in linear coordinates along both axes. One can distinctly see the piecewise-linear dependence $Nu\ Ra = f(Ra)$. The spread of points in the experiments with the upper glass boundary of the layer appears to be larger due to the lesser accuracy, while maintaining and measuring the temperature of the wall, which, in the case of the copper wall, lay within the range 0.01°C during the whole experiment, having been conducted for many hours (up to 16 h). The experiments with the glass wall were conducted in order to find out the possibility of comparing the evolution of the spatial form of the flow and its structure [47–50] with the obtained values of Ra_i, being the boundaries of the discrete transitions (Table 3). In the case of the glass upper boundary, the values of Ra_i practically coincide with those in Table 3.

To compare the results, the experiments were carried out using the same method, as with refs. [47–50]. The transition of the installation to a specified stationary regime of heat transfer, the course of the temperature on the boundaries being uncontrolled according to time, takes place during a time less than or equal to 3 h. Then there is an exposure for 1–2 h, a complete cycle of measurements and a transition to a state with a larger or smaller Ra in a variety of ways. The first way is to change the height of the layer H by the value $\pm\Delta H < 5\%H_0$. After that, there is an exposure for 20 min in one series of experiments and for 1 h in the other. The second way is that for a constant H, after the transition to the stationary regime, the time linear course of the temperature on the lower boundary is switched on towards the growth or drop at the velocity 0.3°C h^{-1}.

In experiments with the 1 h exposure [in Table 3, the results up to $i = 8$ inclusive, and in Fig. 15(a)], all the regions before and after Ra_i were passed as with a number of various $\Delta T = \text{const}$. Within the framework of the experimental error, the results with different ΔT's and a constant H ($Ra = \text{idem}$) turn out to coincide. This is evidence of a weak influence of the parameter L/H, whose monotonous alteration has been shown by experiments.

In experiments with small exposure and variable H's, with the monotonous change of ΔT ($H = \text{idem}$), the results coincide. In these experiments, between the second and the fourth transitions in Table 3, there appear two fractures for $Ra_{3,\text{add}} = 4.8 \times 10^3$ and $Ra_{4,\text{add}} = 8.6 \times 10^3$, the tangents of inclination angles being smaller within the intervals between the neighbouring fractures.

The discrete transitions $i = 9$–14 in Table 3 were obtained according to the measurement results, when the stationary regime had been maintained for 9–12 h after its establishment. In these experiments, the data concerning the statistical properties of the temperature field, for a number of Ra values, were obtained at a time.

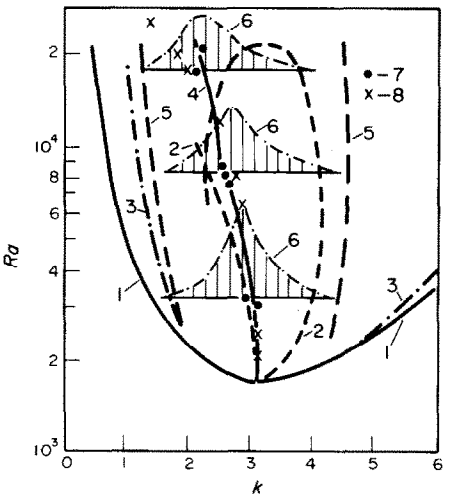

FIG. 16. Diagram of convective rolls stability: 1, equilibrium stability neutral curve; 2, neutral curves, limiting convective rolls stability domain; 3, domain of hydrodynamical stability with two-dimensional roll convection; 4, experimentally obtained average values of wave number; 5, averaged boundaries of experimentally observed values of wave numbers; 6, wave numbers probabilities distribution curves; 7, mean values of wave numbers, $H = 3.15$ mm; 8, mean values of wave numbers obtained by Krishnamurti [53].

Comparing the results of the conducted experiments, one may arrive at the conclusion that the values of Ra_i are largely determined by the rate of the alteration of Ra and slightly depend upon the way of its change. Different ways of changing Ra are accompanied by introducing perturbations of various nature (hydrodynamical, with the change of H, as well as thermal, with the change of ΔT) and with various times of attenuation into the system, however, if one judges by the integral characteristics, the system does not sense them. Therefore, there exist the times of rebuilding the structure of the convective flow itself, its relaxation times beings considerably larger than those of the introduced attenuation perturbations.

The obtained Ra values correlate with the complications of the stationary spatial form of the flow up to $i \leqslant 6$, as fast as Ra grows [47, 50]. The first transition for $Ra \approx 1700$ is connected with the appearance of the roll form of the flow after the mechanical equilibrium stability has been lost. Within the range of Ra approximately up to Ra_2 (Table 3), the spread of the rolls turns out to conform to the length of the wave (Fig. 16), however, they happen to be straight, their generatriscs being almost parallel (alternating sinking and lifting flows). Within the range from $\sim Ra_2$ up to $\sim Ra_4$, the characteristic form is considered to be a quasi-two-dimensional stationary roll structure with spatial modulation of the wavelength. In the domain from $\sim Ra_3$ to $\sim Ra_4$ one may observe a three-dimensional pattern with characteristic wedging-ins and separations of the rolls. Within the range from Ra_4 to Ra_5, slow drifting of the flow structure in the horizontal plane may be observed and a developed secondary flow in the form of short cross rolls exists near the horizontal boundaries. For $Ra \gtrsim Ra_5$, the main roll-like flow is practically destroyed and a polygonal structure of irregular form with a superimposed small-scale secondary flow can be observed. The time dependence becomes more pronounced, the cell structure oscillates near a certain equilibrium position with a period of 1 min. As fast as Ra grows, the spatial complication of the form of the

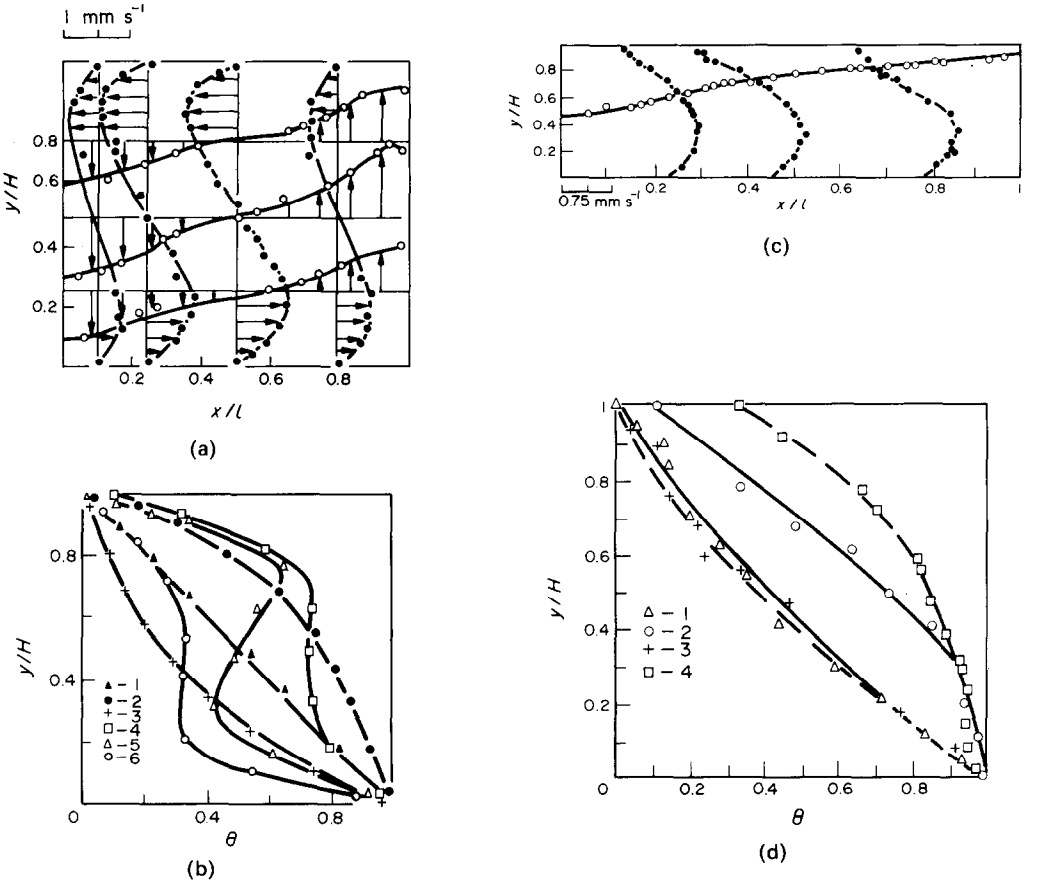

FIG. 17. Velocity and temperature distribution fields in different cells. (a), (b) Two rigid walls—roll planeform cells: (a) $H = 3.15$ mm, $l = 3.6$ mm, $Ra = 8.77 \times 10^3$, $U_m = 0.77$ mm s^{-1}, $\bar{T} = 33.7$°C, $\Delta T = 2.67$°C; (b) 1, $Ra = 1580$, $H = 3.15$ mm, $\Delta T = 0.72$°C, $Ra = 2.5 \times 10^3$, $H = 2.55$ mm, $\Delta T = 2$°C; 2, upward flow ($x/l = 1$); 3, downward flow ($x/l = 0$), $Ra = 8.68 \times 10^3$, $\Delta T = 3.75$°C, $T = 21.64$°C, $H = 3.15$ mm; 4, $x/l = 0.94$; 5, $x/l = 0.27$; 6, $x/l = 0$. (c), (d) Upper boundary is free-polygonal planeform cells: (c) $H = 2.58$, $l = 6.77$ mm, $\Delta T = 0.36$°C, $Ra = 600$, $Ma = 840$, $Bi = 0.26$; (d) 1, $x/l = 0$; 2, $x/l = 1$, $Ra = 300$, $Ma = 730$, $Bi = 0.26$, $H = 2.12$ mm, $\Delta T = 0.38$°C; 3, $x/l = 0$; 4, $x/l = 1$.

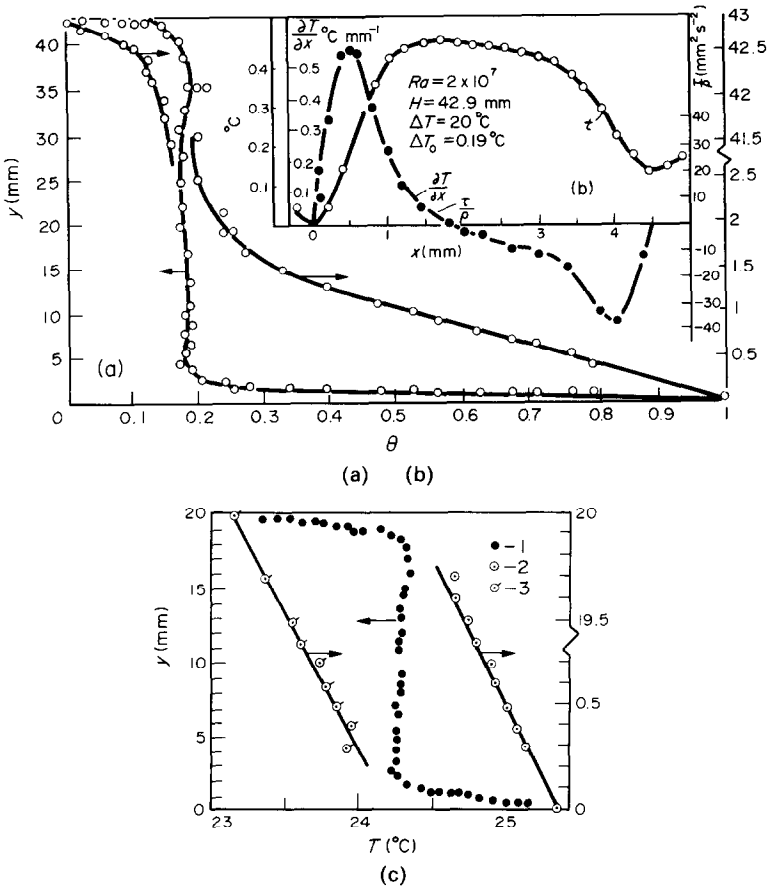

FIG. 18. Mean temperature profiles for horizontal layers: (a) upper free boundary, $Ra = 2 \times 10^7$, $Bi = 0.95$, $H = 42.9$ mm, $\Delta T = 2°C$; (b) profile of temperature along free boundary and thermocapillary distribution within the range of a small-scale subsurface cell; (c) two rigid walls, $Ra = 1.53 \times 10^6$, $H = 20$ mm, $\Delta T = 2.93°C$.

flow turns out, first of all, to be more pronounced, after which its time behaviour complicates.

As fast as Ra grows, successive reconstruction of the velocity and temperature fields in separate cells takes place and the horizontal dimension of the cells increase (Fig. 16). Within the limits of a separate vortex along the horizontal boundaries, the dynamic [Fig. 17(a)] and thermal [Fig. 17(b)] boundary layers develop. The appearance of the secondary flow takes place simultaneously near the horizontal layers and seems to be connected with the thermogravitational instability in instably stratified boundary layers [Curves 4–6 in Fig. 17(b)].

The experiments carried out on visualized liquid show that the cell flow with horizontal dimensions $\sim H$ remains up to $Ra \lesssim 2 \times 10^8$ [40, 43–45]. For large Ra, these cells move in the horizontal plane and change their shape and size therein. The conservation of the large-scale cell structure affects the mean temperature distribution according to the height of the liquid layer (Fig. 18). A weak temperature gradient, inverse to the initial one, remains in the core up to $Ra \lesssim 10^7$ [47–50].

In the case of the free upper boundary, its non-isothermality and the dependence of the liquid surface tension coefficient σ on temperature favour the manifestation of the thermocapillary effect. This effect causes tangential tensions along the free surface, from its more heated part to the cold part. Thermocapillarity makes the liquid move in the same direction, as with the thermogravitational effect.

In thin (in ref. [45] $\leqslant 6$ mm) layers with a free upper boundary, the critical value of the temperature drop being less than with two rigid isothermal boundaries, convective movement of the polygonal spatial form develops. The polygonal cells, the lifting flow in the center and the random distribution of the dimensions l_x and l_y are of irregular form. The intensity of the movement considerably increases, as with two rigid boundaries, their temperature drop and the height of the layer being the same, which one can conceive by comparing the data in Fig. 17.

It was shown in refs. [48–50] that the thermocapillary mechanism also considerably affects the heat transfer processes in the turbulent regime ($Ra \geqslant 10^6$) for large heights of the layer, by forming a near-surface vortex layer and intensifying the transfer processes near the free surface of the liquid. The mean temperature profile in a layer with a free boundary is given in Fig. 18. Its shape differs considerably in the intensity of the heat transfer near the horizontal boundaries of the layer.

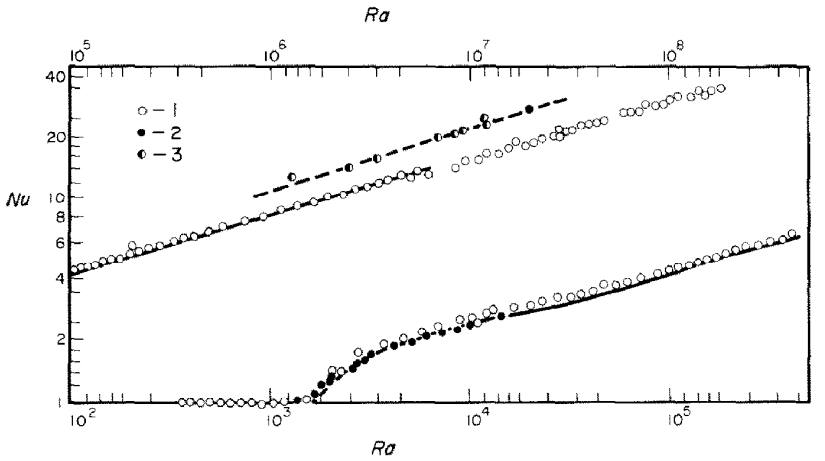

FIG. 19. Dependence of non-dimensional heat transfer coefficient Nu on Ra ($Pr \cong 16$): 1, 2, two rigid walls (copper–copper, copper–glass, respectively); 3, upper free boundary ($Bi = 0.95$), solid line refers to ref. [63].

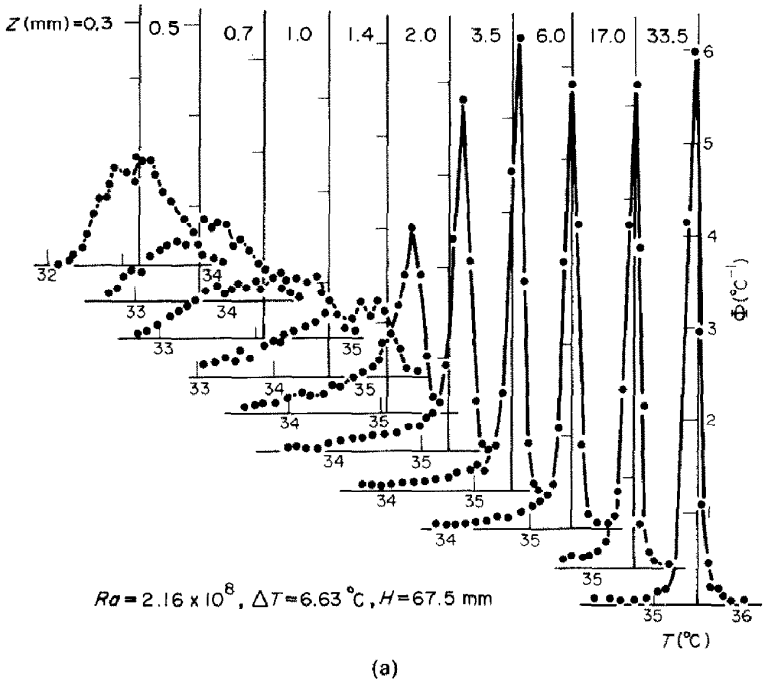

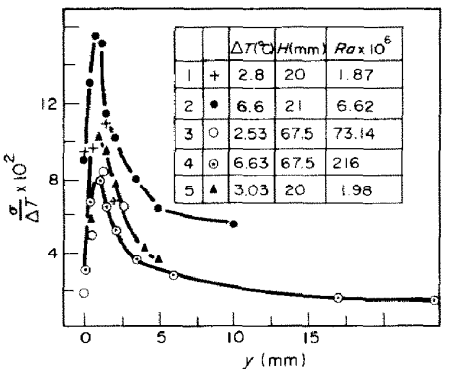

FIG. 20. (a) Selected estimates of temperature instantaneous local drops probability density, $Ra = 2.16 \times 10^8$, $\Delta T = 6.63°C$, $H = 67.5$ mm; (b) intensity of temperature fluctuations (according to ref. [52]).

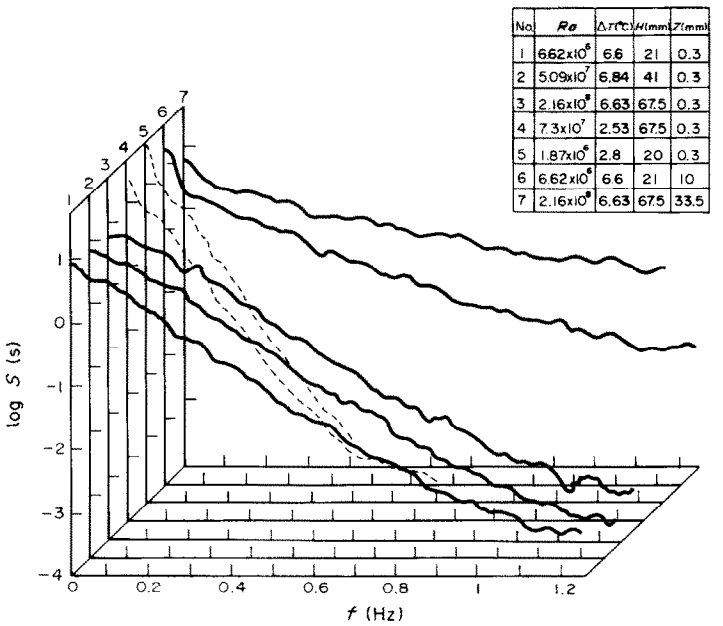

FIG. 21. Selected estimates of temperature fluctuations spectral density in horizontal layer with two rigid walls (according to ref. [52]).

The 'boundary core' temperature drop near the free surface ΔT_x is almost 3-fold lower than with the lower rigid one ΔT_r. As fast as Ra grows, the ratio $\Delta T_x/\Delta T_r$ increases and the inverse temperature gradient in the core disappears [Fig. 18(a)]. In a layer with two rigid walls, the temperature profiles appear to be mirror antisymmetrical, the temperature drop near the boundaries being the same. In the experiments on water layers with a free boundary, upon which impurities can be properly absorbed, with the result that the thermocapillary effect is suppressed, the profiles appear to be also symmetrical [50].

In Fig. 18(b), a fragment of an analogous record of a signal from a thermocouple, placed on a free surface, is shown. Such signals, obtained synchronously with a large-scale shooting of that part of the liquid free surface, where the fixed thermocouple has been placed, allow us to obtain the longitudinal surface distribution of temperature within the range of small-scale cells and estimate the thermocapillary tangential tension (being equal to the friction τ/ρ in Fig. 18(b)).

In Fig. 19 the data according to the values of the heat transfer coefficients for a layer with two rigid walls, which were measured in refs. [50, 52], as well as for free surface layers [50], are given. One can see that with the turbulent regime, the values of Nu in the free boundary layer and the thermocapillarity effect are almost 30% higher than in the layer with rigid walls.

In Figs. 20 and 21, some results of the investigations concerning the statistical properties of the temperature field in layers with two rigid walls are presented. The given results show the similarity in the behaviour of the temperature fluctuations near variously oriented boundaries. The behaviour of the intensities of the temperature fluctuations [Figs. 1 and 20(b)] and the probability density chosen estimates of instant local temperature drops [Figs. 20(a) and 7 in ref. [33]] according to the boundary-layer depth, appears to be qualitatively similar. The chosen estimates of the spectral density temperature fluctuations (Figs. 21 and 4) also show the similarity of the behaviour of the temperature fluctuations, i.e. while moving from the wall, Ra = idem, or with the growth of Ra, y = idem, the raising of the high frequency part of the spectrum occurs. The turbulent convection in the horizontal layer differs in that the highest frequency of the fluctuations $f_B \sim 1$ Hz for $Pr = 16$ is lower by an order of magnitude than the frequency in the vertical layer.

For the above-mentioned reasons, the processes (mechanisms) of the transition of the laminar thermogravitational flow into the turbulent one seem to be more complicated as compared with the isothermical forced flow. For those very reasons experimental investigations are less readily available. However, there also exist some advantages. First of all, there is the possibility of arranging the flow with a very low level of the 'travelling flow turbulence'. Secondly, the processes of the transition to turbulent flow seem to be of gradual, phase nature for all kinds of flows, which appears to be more pronounced in thermogravitational flows.

These examples might help you to more thoroughly investigate the peculiarities of gradually complicating the structure of the flow at separate stages of its transition into the turbulent one. It is evident that at present thermogravitational flows have not been sufficiently investigated.

REFERENCES

1. R. J. Schmidt and O. A. Saunders, Motion of a fluid heated from below, *Proc. R. Soc., London* **165A**(921), 216–228 (1938).
2. O. A. Saunders, Natural convection in liquids, *Proc. R. Soc., London* **172A**(948), 55–71 (1939).
3. S. S. Kutateladze, Some considerations on heat transfer in a free flow, *Zh. Tekh. Fiz.* **5**, 1706–1710 (1935).
4. S. S. Kutateladze, *Fundamentals of Heat Transfer (Osnovy Teorii Teploobmena)*. Atomizdat, Moscow (1979).
5. S. S. Kutateladze, *Pristennaya Turbulentnost.* Nauka, Novosibirsk (1973).
6. S. S. Kutateladze, Razvitie osnovnykh idey teorii turbulentnosti, *Vop. Istor. Estest. Tekh.* No. 4, 112–116 (1980).
7. G. Z. Gershuni and E. M. Zhukhovitskiy, *Convective Stability of an Incompressible Fluid.* Nauka, Moscow (1972).
8. G. Z. Gershuni and E. M. Zhukhovitskiy, Convective stability, in *Itogi Nauki i Tekhniki. Mekhanika Zhidkosti i Gaza*, Vol. 11, pp. 66–154. Moscow (1978).
9. E. Griffiths and A. H. Davis, The transmission of heat by radiation and convection, Dept. of Scientific and Industrial Research, Special Rep. No. 9, British Food Investigation Board, London (1922).
10. E. Schmidt and W. Beckman, Das Temperatur- und Geschwindigheitsfeld von einer Wärme abgebenden senkrechten Platten bei natürlicher Konvektion, *Tech. Mech. Thermo-Dynam.* **1**(10), 341–349 (1930).
11. H. Schlichting, *Grenzschicht-Theorie, Fünfte erweiterte und neubearbeitete Auflage.* Verlag G. Braun, Karlsruhe (1964).
12. B. Gebhart, Natural convection flows and stability, in *Advances in Heat Transfer*, Vol. 9, pp. 273–348. Academic Press, New York (1973).
13. B. Gebhart, Instability, transition and turbulence in buoyancy-induced flows, in *Annual Review of Fluid Mechanics*, Vol. 5, pp. 213–246. Palo Alto, California (1973).
14. A. G. Kirdyashkin, Struktura teplovykh techeniy u poverkhnosti teploobmena, in *Modeli v Mekhanike Sploshnoy Sredy*, pp. 69–90. Novosibirsk (1979).
15. E. R. G. Eckert and T. W. Jackson, Analysis of turbulent free convection boundary layer on flat plate, *NACA Rep.* **1015**, 7 (1951).
16. O. A. Plumb and L. A. Kennedy, Application of a K-turbulence model to natural convection from a vertical isothermal surface, *Trans. Am. Soc. Mech. Engrs*, Series C, *J. Heat Transfer* **99**(1), 79–85 (1977).
17. S. S. Kutateladze, A. G. Kirdyashkin and V. P. Ivakin, Turbulent natural convection on a vertical plate and in a vertical layer, *Int. J. Heat Mass Transfer* **15**(2), 193–202 (1972).
18. S. S. Kutateladze, A. G. Kirdyashkin and V. P. Ivakin, Turbulent natural convection on an isothermal vertical plate, *Teplofiz. Vysok. Temp.* **10**(1), 91–95 (1972).
19. S. S. Kutateladze, A. G. Kirdyashkin and V. P. Ivakin, Turbulent natural convection on an isothermal plate, *Dokl. Akad. Nauk SSSR* **6**, 1270–1273 (1974).
20. S. S. Kutateladze, A. G. Kirdyashkin and V. P. Ivakin, Turbulent natural convection on a vertical plate, in *Sovremennye Problemy Gravitatsionnoy Konvektsii*, pp. 3–11. Minsk (1974).
21. V. P. Ivakin, A. G. Kirdyashkin and L. I. Chernyavskiy, Investigation of turbulent boundary layer structure with natural convection near a vertical plate, in *Wall Turbulent Flow*, Part 2, pp. 256–269. Novosibirsk (1975).
22. R. Cheesewright, Turbulent natural convection from a vertical plane surface, *Trans. Am. Soc. Mech. Engrs*, Series C, *J. Heat Transfer* **90**(1), 1–8 (1968).
23. A. I. Leontyev and A. G. Kirdyashkin, Experimental study of free convection in horizontal and vertical layers, in *Teplo-i Massoperenos, Energie*, Vol. 1, pp. 661–664. Moscow (1968).
24. A. G. Kirdyashkin and A. G. Leontyev, Investigation of hydrodynamics and heat transfer in vertical layers of fluids under free convection conditions, *Teplofiz. Vysok. Temp.* **7**(5), 940–945 (1969).
25. A. G. Kirdyashkin, A. G. Leontyev and N. V. Mukhina, Stability of laminar fluid flow in vertical layers under free convection conditions, *Izd. Akad. Nauk SSSR, Mekh. Zhidk. Gaza* No. 5, 170–174 (1971).
26. A. G. Kirdyashkin and N. V. Mukhina, Free convection in inclined layers of fluid with step-like dependence of heat exchange surface temperature, *Zh. Prikl. Mekh. Tekh. Fiz.* No. 6, 115–121 (1971).
27. A. A. Predtechenskiy, A. G. Kirdyashkin and V. S. Berdnikov, Stability of free convection liquid flow in an inclined flat lay, in *Sovremennye Problemy Teplovoy Gravitatsionnoy Konvektsii*, pp. 12–18. Minsk (1974).
28. A. G. Kirdyashkin and A. A. Predtechenskiy, Stability of boundary layer regime with free convection in a vertical flat slot, in *Problemy Teplofiziki i Fizicheskoy Gidrodinamiki*, pp. 111–119. Nauka, Novosibirsk (1974).
29. N. V. Mukhina and A. A. Predtechenskiy, Wave secondary flows with free convection of air in a vertical slot, in *Some Problems of Hydrodynamics and Heat Transfer*, pp. 29–36. Novosibirsk (1976), (in Russian).
30. A. A. Predtechenskiy, Self-excitation of thermo-convective waves in a vertical liquid layer heated from aside, in *Thermophysical Investigations*, pp. 29–34. Novosibirsk (1977), (in Russian).
31. A. A. Predtechenskiy, The stability of free convection in a vertical fluid layer, *Inst. Thermophys. Acad. Sci. USSR Sib. Dep.*, Preprint No. 19–77 (1977), (in Russian).
32. S. S. Kutateladze, V. P. Ivakin, A. G. Kirdyashkin and A. N. Kekalov, Turbulent free convection in a vertical layer, *Teplofiz. Vysok. Temp.* **15**(3), 545–553 (1977).
33. A. G. Kirdyashkin, V. I. Semenov, V. S. Berdnikov and V. A. Gaponov, The structure of temperature field in a vertical layer with thermal gravitational convection, *Teplofiz. Vysok. Temp.* **20**(5), 922–928 (1982).
34. A. G. Kirdyashkin and V. I. Semenov, Spectra of temperature fluctuations in a vertical layer with thermal gravitational convection, *Teplofiz. Vysok. Temp.* **21**(4), 731–739 (1983).
35. M. P. Sorokin, Free convection of liquid in a slot, occurring under boundary layer conditions, *J. Engng Phys.* **4**(8), 107–110 (1961).
36. J. W. Elder, Laminar free convection in vertical slot, *J. Fluid Mech.* **23**(1), 77–98 (1965).
37. J. E. Hart, Stability of the flow in a differently heated box, *J. Fluid Mech.* **47**(3), 547 (1971).
38. J. Oshima, Experimental studies of free convection in a rectangular cavity, *J. Phys. Soc. Japan* **30**(3), 872–882 (1971).
39. G. A. Ostroumov, *Svobodnaya Konvektsiya v Usloviyakh Vnutrenney Zadachi.* Gostekhizdat, Moscow–Leningrad (1952).
40. E. R. Eckert and W. O. Carlson, Natural convection in an air layer enclosed between two vertical plates with different temperatures, *Int. J. Heat Mass Transfer* **2**, 106–120 (1961).
41. J. W. Elder, Turbulent free convection in vertical slot, *J. Fluid Mech.* **23**(1), 99–111 (1965).
42. A. V. Getling, Evolution of two-dimensional disturbances in the Rayleigh–Bénard problem and their preferred wavenumbers, *J. Fluid Mech.* **130**, 165–186 (1983).
43. F. H. Busse, Non-linear properties of thermal convection, *Rep. Prog. Phys.* **41**, 1929–1967 (1978).
44. J. A. Whitehead and B. Parsons, Observations of convection at Rayleigh numbers up to 760 000 in a fluid with large Prandtl numbers, *Geophys. Astrophys. Fluid Dynamics* **9**, 201–217 (1978).
45. A. I. Leontyev and A. G. Kirdyashkin, Heat transfer with

free convection in horizontal slots and in large volume above horizontal surface, *J. Engng Phys.* **9**(1), 9–14 (1965).
46. A. I. Leontyev and A. G. Kirdyashkin, Experimental study of flow patterns and temperature fields in horizontal free convection liquid layers, *Int. J. Heat Mass Transfer* **11**(10), 1461–1466 (1968).
47. S. S. Kutateladze, A. G. Kirdyashkin and V. S. Berdnikov, Velocity field in a convection cell in a horizontal layer of fluid in thermal gravitational convection, *Atmosph. Oceanic Phys.* **10**(2), 82–86 (1974).
48. S. S. Kutateladze, A. G. Kirdyashkin and V. S. Berdnikov, Effect of thermocapillary forces on transport processes near free surface of liquid in a horizontal layer with turbulent thermal gravitational convection, *Dokl. Akad. Nauk SSSR* **231**(2), 309–311 (1976).
49. V. S. Berdnikov, Structure of free convection liquid flow at a free heat exchange surface, *Heat Transfer—Sov. Res.* **11**(3), 13–24 (1979).
50. V. S. Berdnikov and A. G. Kirdyashkin, Structure of free convection flows in a horizontal layer of liquid under various boundary conditions, *Fluid Mech.—Sov. Res.* **9**(6), 1–36 (1980).
51. V. A. Markov, Heat transfer through horizontal liquid layer heated underneath, in *Hydrogasdynamics and Heat Transfer in Condensed Media*, pp. 40–45. Novosibirsk (1981), (in Russian).
52. V. S. Berdnikov, V. A. Markov and O. V. Kim, Thermogravitational convection in flat horizontal inclined layers of liquid heated from below, in *The Structure of Forced and Thermogravitational Flows*, pp. 122–146. Novosibirsk (1983) (in Russian).
53. R. Krishnamurti, On the transition to turbulent convection. Part 1. The transition from two- to three-dimensional flow. Part 2. The transition to time-dependent flow, *J. Fluid Mech.* **42**(2), 295–307, 309–320 (1970).
54. W. V. R. Malkus, Discrete transitions in turbulent convection, *Proc. R. Soc.* **225A**(1161), 185–195 (1954).
55. G. E. Willis and J. W. Deardorff, Confirmation and renumbering of the discrete heat flux transitions of Malkus, *Physics Fluids* **10**(9), 1861–1866 (1967).
56. A. M. Garon and R. J. Goldstein, Velocity and heat transfer measurements in thermal convection, *Physics Fluids* **16**(11), 1818–1825 (1973).
57. T. Y. Chu and R. J. Goldstein, Turbulent convection in a horizontal layer of water, *J. Fluid Mech.* **60**(1), 141–159 (1973).
58. R. J. Schmidt and S. W. Milverton, On the instability of a fluid when heated from below, *Proc. R. Soc., London* **A152**(887), 586–594 (1935).
59. M. Jakob, *Heat Transfer*, Vol. 1, p. 758. Wiley, New York (1949).
60. W. Mull and H. Reiher, Der Wärmeschutz von Luftschichten, *Beih. Z. Gesundheitstech., Ing.* Ser. 1, 28 (1930).
61. B. J. Daly, A numerical study of turbulence transitions in convective flow, *J. Fluid Mech.* **64**(1), 129–165 (1974).
62. G. E. Willis, J. W. Deardorff and R. C. J. Somerville, Roll-diameter dependence in Rayleigh convection and its effect upon the heat flux, *J. Fluid Mech.* **54**(2), 351–367 (1972).
63. P. L. Silveston, Wärmedurchgang in waagerechten Flüssigkeitsschichten, *Forsch. Geb. IngWes.* **24**, 24–32, 59–69 (1958).